

A medium resolution double crystal based small-angle neutron scattering instrument at Trombay

S. Mazumder*, D. Sen, T. Saravanan and P. R. Vijayaraghavan

A double crystal-based moderate resolution small-angle neutron scattering instrument has been built and commissioned at the guide laboratory of Dhruva reactor, Bhabha Atomic Research Centre, Trombay, India. The instrument consists of a non-dispersive (1, -1) setting of 111 reflections of silicon single crystals with the sample between the two crystals. The neutron wavelength used is 0.312 nm. At 65 MW of reactor power, the peak count rate of the blank rocking curve is about 55 counts per second at the detector position and the ratio of integrated signal to integrated noise is ~ 450 for a typical experiment with sintered alumina. The accessible range of wave vector transfer q is found to be 0.003–0.173 nm⁻¹, which corresponds to a range of resolvable real-space dimension of 2000–40 nm, for these specimens. The instrument is calibrated with respect to the high resolution ultra small-angle neutron scattering instrument S18 at the Institute Laue–Langevin in Grenoble, France.

THE importance and usefulness of the small-angle neutron scattering (SANS) technique is increasingly being realized as its applications in different materials science problems are growing by leaps and bounds. Conventional slit collimation instruments equipped with two-dimensional position-sensitive detectors are widely used for investigating problems in materials science and biology. The typical maximum accessible length scale for a slit collimation instrument is ~ 10² nm. But large inhomogeneities as commonly encountered in cements, ceramics, macromolecules and magnetic domains are beyond the resolution limit of the conventional slit collimation instrument, where collimation is performed in real space by slits. For investigations involving higher length scales, slit collimation instruments, with a few exceptions, such as D11 (ILL, Grenoble), become inefficient and impracticable owing to the necessity of employing long flight paths and small beam cross-sections.

To access larger length scales, a non-dispersive (1, -1) double crystal (DC)-based instrument is used. The instrument uses two parallel single crystals of high perfection. The very sharp Bragg condition of these crystals defines the q -resolution. The sample is placed between the two crystals and the scattering profiles of the specimens are recorded by rotating one crystal against the other. This

type of instrument is known as Bonse–Hart camera¹ in X-ray diffraction. In a DC-based instrument, unlike the slit collimation instrument, the collimation is performed in the reciprocal space only by crystals and the resolution in wave vector transfer, q , is independent of the beam cross-section. Because of the non-dispersive setting of both the crystals, the width of the rocking curve is independent of the divergence of the incoming beam. The high q -resolution exists in one dimension only and the recorded data are to be subjected to resolution corrections. The instruments can be compact and do not require long flight paths and two-dimensional position-sensitive detectors as the data are recorded through a step-by-step rotation of the analyser crystal. DC-based SANS instruments are relatively much cheaper vis-a-vis slit collimation instruments.

However, due to the necessity of recording of scattering intensity through a step-by-step rotation of the analyser crystal, measurement time is rather long. Further, the sensitivity of the instrument is poor at high q vis-à-vis slit collimation instrument, due to a background caused by diffuse scattering from the crystal surfaces. Use of mosaic crystal as analyser or monochromator enhances luminosity for higher values of q , but it is applicable to strongly-scattering systems because of the rather high background level caused by the long tails of the mosaic-spread distribution curves and diffuse scattering.

There are a large number of DC-based SANS diffractometers around the world. In recent times, this type of

The authors are in the Solid State Physics Division, Bhabha Atomic Research Centre, Trombay, Mumbai 400 085, India.

*For correspondence. (e-mail: smazu@apsara.barc.ernet.in)

facility has found fruitful applications in ceramics and cements².

In this article, the performance of a newly developed moderate resolution DC-based SANS instrument (MSANS) at Trombay is reported.

An algorithm to extract scattering mean free path from two recorded scattering profiles

To diagonalise multiple scattering, it is advised to record two scattering profiles from the same material, either by changing the sample thickness and/or the wavelength by a significant extent. In conventional small-angle scattering, variation of thickness or wavelength, λ , changes the profile with respect to a scale factor only. If the profiles are different, not only in scale but also in shape, then the profiles are said to have different functionality – a thumb impression of multiple scattering. Under these circumstances, it is necessary to extract the true single scattering profile from the recorded profiles having different functionality. An algorithm used for this purpose assumes the scattering medium to be an ‘effective one’³, where the linear dimension of the inhomogeneities is very small in comparison to the scattering mean free path, L , of the radiation inside the sample. The algorithm for the inversion of multiple scattering profile is based on the principle that although different multiple scattering profiles are functionally distinct with $N = (\text{sample thickness}/L)$, the computed single scattering profiles from each of them are functionally same or least deviated, provided the correct N value is used for the inversion. The algorithm provides an estimation of L from two profiles, after background and transmission corrections, recorded with variation of sample thickness or wavelength, for extraction of single scattering profile. Details of the algorithm are given in refs. 4 and 5.

Instrumental parameters of MSANS

Figure 1 shows the schematic layout of the DC-based SANS diffractometer. The instrument has been installed on guide G1 in the guide laboratory of the Dhruva reactor at Trombay. G1, looks at the thermal moderator of the reactor and has cut-off wavelength $\lambda^* = 0.22$ nm (ref. 6). The size of the neutron beam coming from the guide is 2.54 cm (horizontal) \times 10.4 cm (vertical). Two perfect silicon crystals (diameter 8.25 cm and thickness 0.6 cm) cut parallel to (111)-planes are used as monochromator and analyser. The monochromator crystal reflects neutrons with wavelength $\lambda = 0.312$ nm and $\Delta\lambda/\lambda \approx 1\%$. The horizontal angular divergence of neutron beam from the guide is wavelength-dependent and the numerical value of the angular divergence in degrees approximates the numerical value of λ expressed in nm. The horizontal angular divergence of the neutron beam from the guide of

wavelength $\lambda = 0.312$ nm is 0.312° . The monochromator crystal is set on a goniometer.

The monochromatic neutron beam from the monochromator then passes through a one-metre long cadmium collimator, 2 cm \times 5 cm, placed 20 cm away from the monochromator centre. In most of the measurements, a circular beam of 1.5 cm diameter is used. However, depending upon the sample size, provision has been made to vary the beam cross-section. The distance between the monochromator centre and the sample mount centre is 128 cm. The analyser crystal, placed 100.5 cm away from the sample, is set on a precise goniometer with smallest control step size of 0.0012° . The (111) symmetric reflections are used for both the crystals. Neutrons are detected by a BF_3 counter of 3.81 cm diameter, placed 55 cm away from the centre of the analyser crystal.

For measurements of intensity of the primary monochromatized beam and specimen transmission, another BF_3 counter located behind the analyser crystal along the monochromatic beam direction is used. The minimum count-rate at this detector corresponds to the maximum count-rate of the main detector when the analyser is in the Bragg position. This correspondence is used for an independent determination of the exact Bragg angle. The diameter of the aperture before the second detector, placed 160 cm away from the centre of the analyser crystal, is 1 cm.

Performance and calibration of the instrument

For the calibration of MSANS, three sintered alumina specimens have been chosen as secondary standards. The specimens are chemically stable, easy to handle and can be used as standard for any future calibration. To carry out the calibration of the instrument, SANS measurements have been carried out on two instruments, namely at the MSANS, Trombay and also at the ultra small-angle neutron scattering facility (USANS)⁷ S18 of Institute

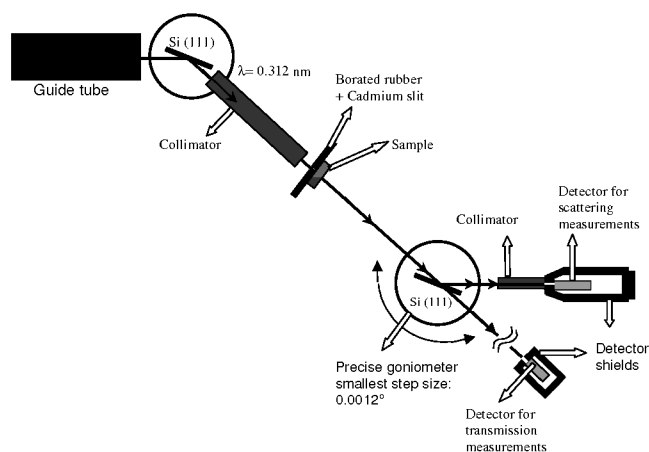


Figure 1. Schematic layout of MSANS, Trombay.

Laue–Langevin (ILL), on the three sintered alumina specimens. The wavelength λ used for the measurements at S18 was 0.187 nm.

The difference in two wavelengths poses a problem as far as the calibration is concerned, and will be dealt with in the present section. This is because the inhomogeneities accessed by high- and moderate-resolution instruments are quite large and scattering data are more often affected by multiple scattering³. This is particularly so because sample thickness cannot be brought down indefinitely due to some practical reasons. It is important to note that in conventional small-angle scattering, where single scattering approximation holds, variation of sample thickness or wavelength does not change the profile, i.e. the profiles are different by a scaling factor only.

Description of calibration specimens

Sintered alumina specimens of right cylindrical geometry of nearly 1.44 cm diameter and different thicknesses of 0.650, 0.306 and 0.272 cm are prepared by cutting a sintered billet with a diamond saw. Bulk density of the sintered billet, determined by the liquid displacement method using xylene as the suspending liquid, is found to be 3.63 gm/cm³ (91% of theoretical density).

Transmission measurements

For a sample undergoing only small-angle scattering and absorption, transmission $T(\lambda)$ is given by the relation;

$$T(\lambda) = \exp\{-N(\lambda) - \mu(\lambda)t\}, \quad (1)$$

where t is the thickness of the specimen with linear absorption coefficient μ and $N (= t/L)$ is the ratio of sample thickness t to scattering mean free path L . As N and μ are wavelength-dependent, transmission is also wavelength-dependent. When λ is expressed in nm, for alumina specimens with 91% theoretical density, linear absorption coefficient μ can be expressed in the following form,

$$\mu \text{ (cm}^{-1}\text{)} = 0.055 * \lambda \text{ (nm)}. \quad (2)$$

In the diffraction limit,

$$N \propto \lambda^2 \text{ or } N = a\lambda^2 \text{ (say)}, \quad (3)$$

where ‘ a ’ is the material constant. For a monodisperse population of spherical scatterers, with number density ρ of radius R , having same scattering length density contrast D , ‘ a ’ is given by³,

$$a = 2\pi\rho D^2 R^4. \quad (4)$$

It is possible to get an estimate of ‘ a ’ from transmission measurement at λ , as μ is defined for a particular λ . From transmission T_1 measured at a wavelength λ_1 , the expected transmission value T_2 for a wavelength λ_2 is given by the following relation,

$$T_2 = T_1 \exp\{a(\lambda_2^2 - \lambda_1^2) + t(\mu_2 - \mu_1)\}. \quad (5)$$

The measured transmission values of the specimens at the two instruments, denoted by $T_{0.187}$ and $T_{0.312}$, are listed in Table 1. The calculated transmission values of the specimens for neutrons with $\lambda = 0.312$ nm, from measured $T_{0.187}$ values, are denoted by $T_{0.312}^{\text{calc}}$.

It is observed from the Table 1 that $T_{0.312}$ values are more, by ≈ 4 –8%, than those of $T_{0.312}^{\text{calc}}$ values. Thicker the specimen more is the difference between the estimated and experimental values. Transmission as measured in the experiment is always somewhat more because of the contamination of scattering signal with true transmitted component of radiation passing through the sample, due to various factors. But the estimation of true transmission from measured values is quite involved and beyond the scope of the present work. However, it does not affect the measurement of scattering profiles to any significant level because scattering profiles are recorded in the domain of q , where the direct beam contribution is negligibly small.

Scattering measurements

Figure 2 shows scattering profiles, recorded at S18, of ILL of the three specimens. The intensities were corrected for sample absorption and smearing effects. The intensities of the individual scattering profiles are normalized at the lowest q -value accessed in these measurements. It is

Table 1. Measured transmission and the estimated Porod exponents. Measured transmissions, $T_{0.187}$ and $T_{0.312}$, are for the three specimens at the two facilities, namely S18, ILL and MSANS, Trombay respectively. Calculated transmission values of the specimens for neutron beam with $\lambda = 0.312$ nm, from measured $T_{0.187}$ values, are denoted by $T_{0.312}^{\text{calc}}$. η denotes the exponent estimated from the profiles, after background and resolution corrections, recorded at S18, ILL. η' denotes the exponent estimated from the profiles recorded at MSANS, after background and resolution corrections

Sample thickness (cm)	$T_{0.187}$ (%)	$T_{0.312}^{\text{calc}}$ (%)	$T_{0.312}$ (%)	η	η'
0.272 ± 0.001	94.98 ± 0.19	86.84 ± 0.73	91.1 ± 1.3	3.99 ± 0.28	4.05 ± 0.35
0.306 ± 0.001	92.89 ± 0.19	81.64 ± 0.46	87.0 ± 1.2	4.01 ± 0.28	4.01 ± 0.31
0.650 ± 0.001	78.99 ± 0.16	52.28 ± 0.29	60.3 ± 1.3	3.98 ± 0.32	3.99 ± 0.31

observed that the scattering profiles are sample thickness-dependent, indicating the presence of multiple scattering. Further, with increasing sample thickness the scattering profiles become smoother as scattering increases with sample thickness for weakly-absorbing systems.

Porod exponents η estimated from $\ln(\text{intensity})$ vs $\ln(q)$, in the q range beyond $q = 0.018 \text{ nm}^{-1}$ for various specimens are listed in Table 1. The scattering profiles in the q range $q \geq 0.018 \text{ nm}^{-1}$, follow a power law $\sim q^{-4}$ independent of multiple scattering.

To begin with the treatment of the scattering data affected by multiple scattering, we assume the scattering medium to be an effective one. Since profiles from the thinner samples are less affected by multiple scattering, two profiles from specimens of thicknesses 0.272 and 0.306 cm respectively, are chosen for the estimation of

the scattering mean free path L , using an algorithm in refs 4 and 5. The mean free path L for the specimens has been estimated to be $0.064 \pm 0.007 \text{ cm}$.

With $L = 0.064 \pm 0.007 \text{ cm}$, the single scattering profile estimated from the profile of 0.272 cm thick specimen under effective medium approximation is shown in Figure 3. It is expected that the estimated single scattering profile will be sharper compared to the recorded profiles affected by multiple scattering. The unsmooth nature of the data in Figure 3 at some places is due to the unsmooth nature of the recorded profile of the 0.272 cm thick specimen. The inversion of multiple scattering profile to single scattering profile results in increasing unsmoothness and statistical error bars. The single scattering profiles estimated from the profiles of 0.306 and 0.650 cm thick specimens are shown in Figure 4 *a* and *b* respectively.

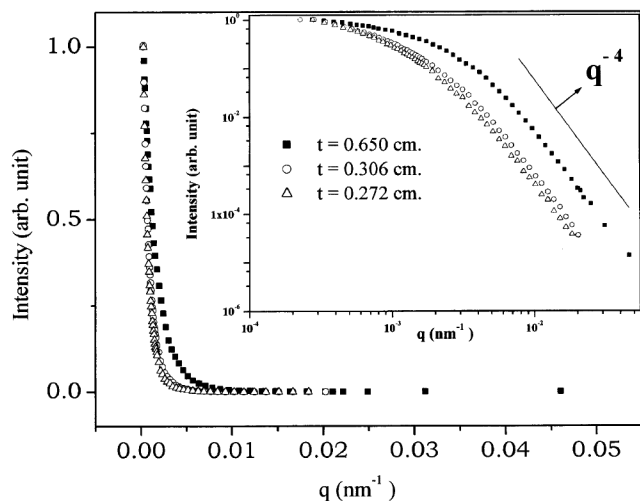


Figure 2. Scattering profiles of the three specimens recorded at S18, ILL. (Inset) Profiles in the log–log scale. A normalized scale has been used. At large q , the profiles follow a power law $\sim q^{-4}$. Error bars are less than the size of the symbols. The solid line is only a guide to the eye.

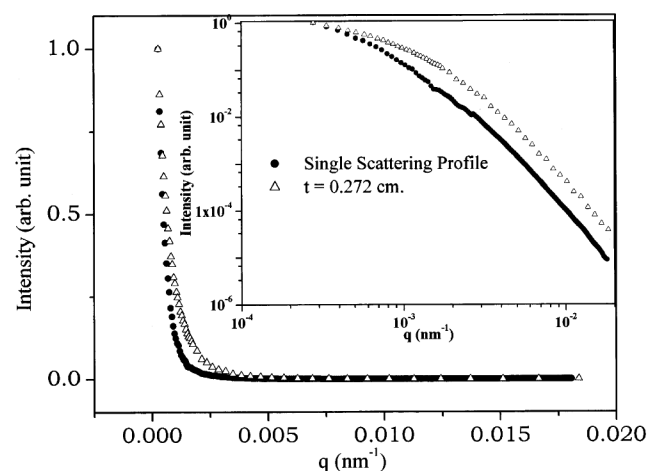


Figure 3. Estimated single scattering profile and recorded profile from specimen of thickness 0.272 cm. (Inset) Profiles in log–log scale. Error bars are less than the size of the symbols.

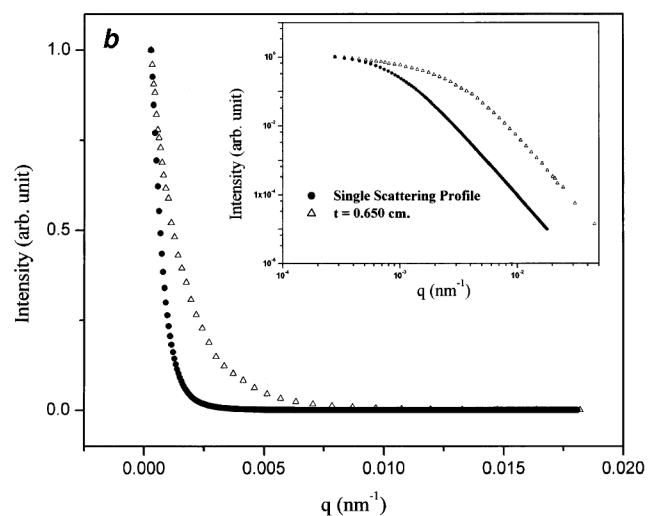
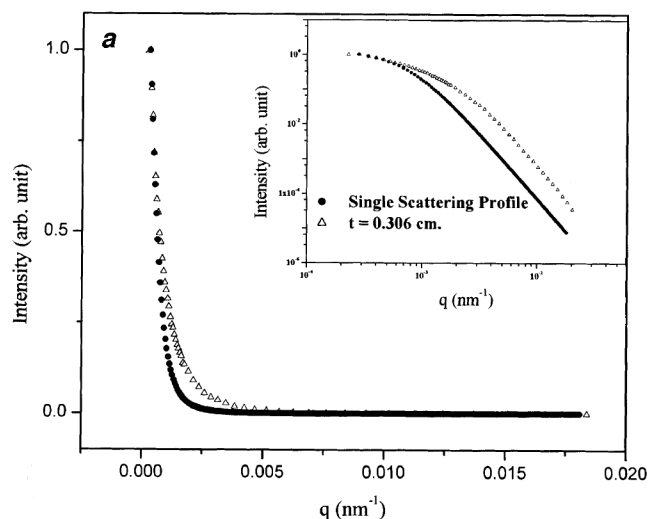


Figure 4. Estimated single scattering profile and recorded profile from specimen of thickness (*a*), 0.306 cm; and (*b*), 0.650 cm. (Inset) Profiles in log–log scale. Error bars are less than the size of the symbols.

With the estimated L and the single scattering profile, the expected scattering profile including contributions from multiple scattering from specimens of thicknesses 0.272, 0.306 and 0.650 cm respectively, have been calculated under effective medium approximation (EMA) for probing radiation with wavelength $\lambda = 0.312$ nm. The calculated profiles are shown in Figure 5.

For calibration of the instrument, the calculated scattering profiles, as shown in Figure 5, are resolution-smearred for different parametric values of a model resolution function, which is often approximated to be Gaussian⁸. The resolution-smearred scattering profiles are then compared in the least square sense with the transmission corrected but resolution uncorrected scattering profiles measured at MSANS, Trombay, to get the best possible value of the parameter of the resolution function. For a detailed calibration procedure followed for this instrument, refer to Mazumder *et al.*⁹.

The MSANS data corrected for background and resolution are shown in Figure 6. The estimated Porod exponents η' in the q range beyond $q = 0.03$ nm⁻¹, listed in Table 1, are nearly equal to 4 – a result consistent with the expectations.

For measurement in a DC-based SANS instrument, the absolute scattering cross-section $\frac{d\Sigma}{d\Omega}(q)$ is given by the following relation,

$$\frac{d\Sigma}{d\Omega}(q) = \frac{I(q)}{I_B(0)\Delta\theta_h\Delta\theta_v t}, \quad (6)$$

where $I(q)$ is the transmission and resolution-corrected recorded scattering profile from a specimen of thickness t , $I_B(0)$ is the scattering intensity for the blank measure-

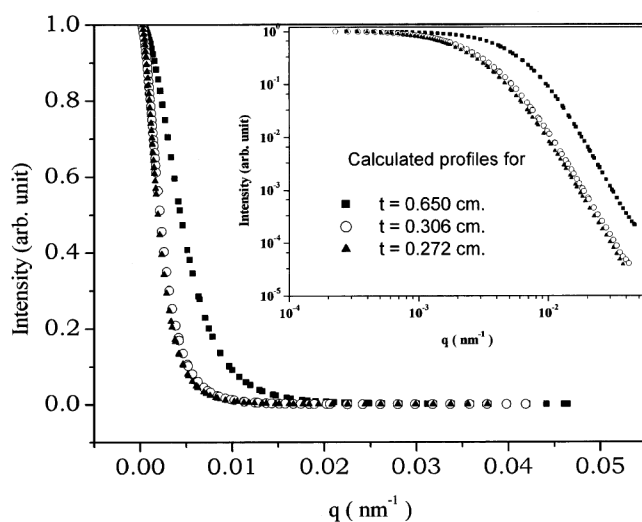


Figure 5. Computed scattering profiles with effective medium approximation for specimens under the consideration that the wavelength of the probing neutrons is 0.312 nm. (Inset) Calculated profiles in log–log scale. Error bars are less than the size of the symbols.

ment at $q = 0$ under the same condition, $\Delta\theta_h$ is the full width at the half maximum (FWHM) of the blank rocking curve in radians and $\Delta\theta_v$ is the ratio of detector aperture in vertical direction to sample-detector distance.

Figure 7 depicts the resolution-corrected scattering profiles of the three specimens, recorded in absolute scale at MSANS, Trombay.

Conclusions

A medium resolution DC-based small-angle neutron scattering instrument at Trombay has been installed and

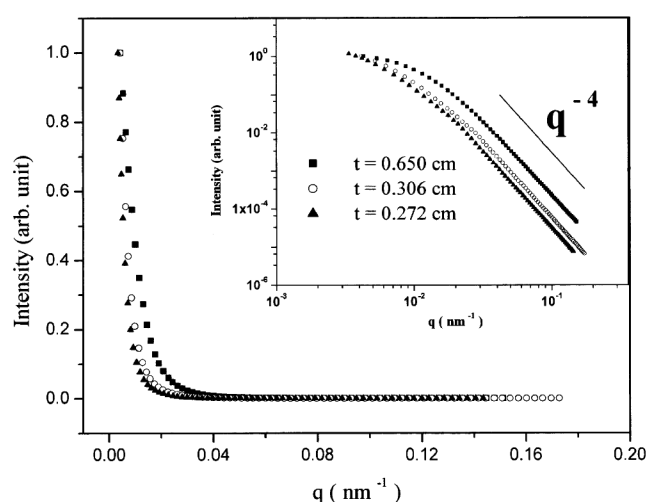


Figure 6. Scattering profiles recorded at MSANS, Trombay, of the three specimens after background and resolution corrections. (Inset) Profiles in the log–log scale. At large q , the profiles follow a power law $\sim q^{-4}$. Error bars are less than the size of the symbols. The solid line is only a guide to the eye.

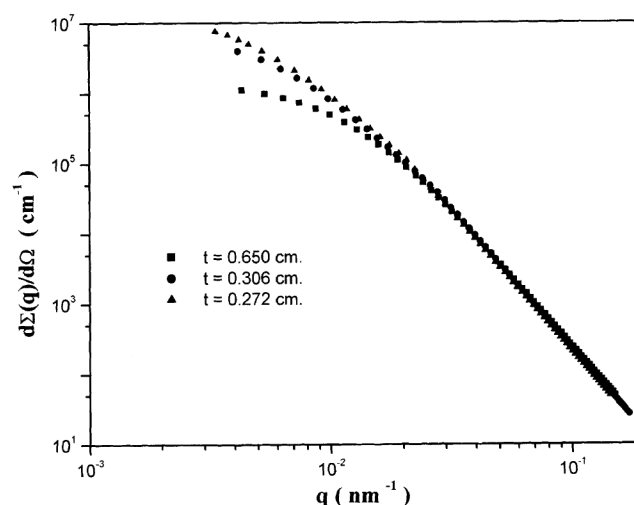


Figure 7. Scattering profiles of the three specimens in absolute scale, recorded at MSANS, Trombay, after resolution corrections. Error bars are less than the size of the symbols.

calibrated. Data have been recorded for three sintered alumina samples. For a typical experiment with sintered alumina, it has been observed that the ratio of integrated signal to integrated noise is 450 and the accessible range of wave vector transfer q is $0.003\text{--}0.173\text{ nm}^{-1}$ – a range which is often of interest in materials science. The instrument will be useful to probe inhomogeneities of linear dimension $2000\text{--}40\text{ nm}$. As far as resolution is concerned, the present instrument is superior to the conventional slit collimation instrument.

Strongly scattering systems like pores in cements and ceramics can be investigated in the newly developed MSANS at Trombay, with reasonably good sensitivity. The instrument has flexibility to access smaller length scale when mosaic crystals are used as analyser. However, due to increased background from crystal imperfections, such configuration will be useful only for strongly scattering systems. Some experimental investigations with hydrating cement paste are underway.

The present facility employs single-bounce flat crystals as monochromator as well as analyser. Use of multi-bounce channel-cut crystals as monochromator and analyser will enhance both the q -resolution and the signal-to-noise-ratio of the experimental data. Work in that direction has already been started.

-
1. Bonse, U. and Hart, M., *Appl. Phys. Lett.*, 1965, **7**, 238–240; Bonse, U. and Hart, M., *Z. Phys.*, 1966, **189**, 151–162.

2. Agamalian, M., Wignall, G. D. and Triolo, R., *J. Appl. Crystallogr.*, 1997, **30**, 345–352; Agamalian, M. *et al.*, *J. Appl. Crystallogr.*, 1998, **31**, 235–240 and the references therein.
3. Mazumder, S. and Sequeira, A., *Pramana – J. Phys.*, 1992, **38**, 95–159; Mazumder, S. and Sequeira, A., *Phys. Rev. B*, 1989, **39**, 6370–6373; Mazumder, S. and Sequeira, A., *Phys. Rev. B*, 1990, **41**, 6272–6277.
4. Mazumder, S., Jayaswal, B. and Sequeira, A., *Physica. B*, 1998, **241–243**, 1222–1224.
5. Jayaswal, B. and Mazumder, S., BARC Report, BARC/1998/E/024, 1998, 1–70.
6. Basu, S. and Rao, L. M., *Physica B*, 1991, **174**, 409–414.
7. Hainbuchner, M. *et al.*, *J. Appl. Crystallogr.*, 2000, **33**, 851–854.
8. Schmidt, P. W. and Hight, R., *Acta Crystallogr.*, 1960, **13**, 480–483.
9. Mazumder, S., Sen, D., Saravanan, T. and Vijayaraghavan, P. R., *J. Neutron Res.*, 2001 (in press).

ACKNOWLEDGEMENTS. We gratefully acknowledge the guidance, continuous support and keen interest of Drs S. K. Sikka, A. Sequeira and M. Ramanadham in this work. We are grateful to Dr S. K. Roy, Materials Science Division, BARC for providing us the alumina specimens used for calibration of the instrument. Help rendered by NPD workshop and Central workshop for fabrication of various components was immense. Access to S18 at ILL, Grenoble is thankfully acknowledged. We are extremely grateful to the referee for reviewing the manuscript thoroughly and for many useful suggestions throughout the manuscript.

Received 13 February 2001; revised accepted 26 April 2001